RECENT OBSERVATIONS, EXPERIMENTS AND SIMULATIONS OF ELECTRON CLOUD EFFECTS AT THE LANL PSR*

Robert J. Macek#, Lawrence J. Rybarcyk, Andrew A. Browman, Jeffery S. Kolski, Rodney C. McCrady, Thomas Spickermann, and Thomas J. Zaugg, LANL, Los Alamos, NM 87544, U.S.A.

Abstract

Recent beam studies were aimed at an improved understanding of the main sources and locations of electron clouds (EC) which drive the observed e-p instability at the Los Alamos Proton Storage Ring (PSR). New results using longitudinal barriers (electron mirrors) to block electrons ejected from the nearby quadrupoles provide definitive evidence that ~75% of the drift space EC signals arise from electrons ejected by ExB drifts from adjacent quadrupole magnets. Modeling of EC generation using a modified version of the POSINST code provides additional insight.

INTRODUCTION

Various electron cloud effects (ECE) have been observed at PSR [1, 2] but the most important is the two-stream e-p instability observed since 1985. Our recent work focused on:

- identifying the locations of the electron clouds driving the instability,
- making use of newly added "electron mirrors" (longitudinal barriers to electron motion) to clearly measure the contribution to the drift space EC by electrons ejected from the adjacent quadrupole magnets and
- resolving a number of issues and puzzles identified in our studies to date.

The location of the strongest EC is important for control of the instability by selective suppression of EC generation. Otherwise, one must use electron suppression everywhere in the ring for effective mitigation.

RECENT STUDIES

Previous studies have indicated that the e-p instability thresholds were insensitive to increases in beam losses. This behavior was verified very cleanly in a recent experiment with a particularly steady beam from the accelerator. We measured the threshold curve i.e., the beam intensity at instability threshold as a function of buncher voltage for nominal losses and shortly thereafter repeated the measurement after changing the foil scattering beam losses a factor of 2 by moving the stripper foil in ~2mm. The resulting threshold curves are plotted in Fig. 1 and show that both threshold curves are virtually identical.

Two-stream instability theory predicts that the threshold should be lower for a higher fractional neutralization of the beam by the EC. The results shown in Fig. 1 suggest that the EC driving the instability saturate at the nominal losses for the intensities used in the threshold curves even though the RFA (retarding field analyzer) signals show a factor of ~2 increase in amplitude [3]. This is a useful reminder that for a long bunch machine, such as PSR, the flux of electrons striking the wall is not a direct measure of the electrons driving the instability. It is the electrons that survive the gap between bunch passages and are captured by the next beam pulse where they oscillate many times (~50 oscillations in one bunch passage) that will drive the instability.

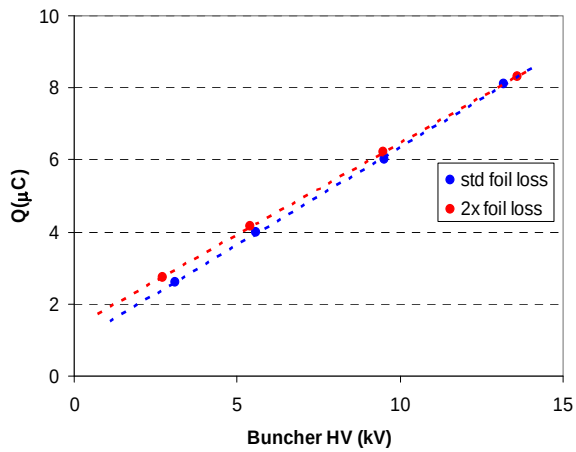

Figure 1: Effect of beam losses on e-p instability threshold curves (data taken 6/26/08).

A low beam loss region of the PSR (section 4) has been instrumented with two special electron cloud diagnostics and two longitudinal electron barriers [4] as shown in the layout of Fig. 2. We designate the electron barriers "electron mirrors" since they reflect (when biased with negative voltage) electrons ejected from nearby quadrupoles. The studies reported here made use of the mirrors and two LANL adaptations of the RFA diagnostic with a sweeping electrode added [1, 5].

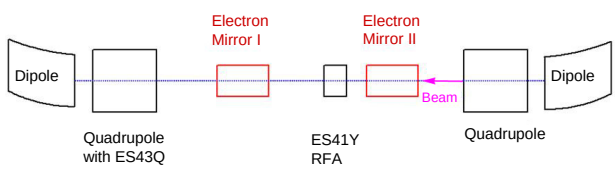

Figure 2: Layout of EC diagnostics in PSR section 4.

The drift space diagnostic is labeled ES41Y and the quadrupole diagnostic, labeled ES43Q, is located in the horizontally defocusing quadrupole at the downstream end of section 4. Both of these diagnostics will measure the flux of electrons striking the chamber walls and, by

*Work supported by DOE SBIR Grant No. DE-FG02-04ER84105 and CRADA No. LA05C10535 between TechSource, Inc. and LANL.
#macek@lanl.gov

pulsing the sweeping electrode at the end of the gap, can also measure the electrons surviving the gap passage.

Results with Electron Mirrors

Analytical calculations and simulations of EC generation in a 3D quadrupole [6] showed that a significant fraction of electrons generated in the quadrupoles are ejected along the beam axis by ExB drifts during passage of the beam pulse. They are ejected with considerable energy, up to 2 keV, into nearby drift spaces and ends of dipoles. To confirm the simulation we developed and installed two longitudinal barriers (electron mirrors) which could be used to isolate the drift space diagnostic from electrons ejected from the nearby quadrupoles.

Several signals from an experiment where the mirrors and the ES41Y sweeper electrode were pulsed for several μs are shown in Fig. 3. The sweeper HV pulse was -500V and the mirrors pulsed at -2kV. There is a reflection in the HV monitor pulse for the sweeper that occurs after an attenuator in the return path. This can safely be ignored since it was not present on the pulse at the electrode and has since been corrected.

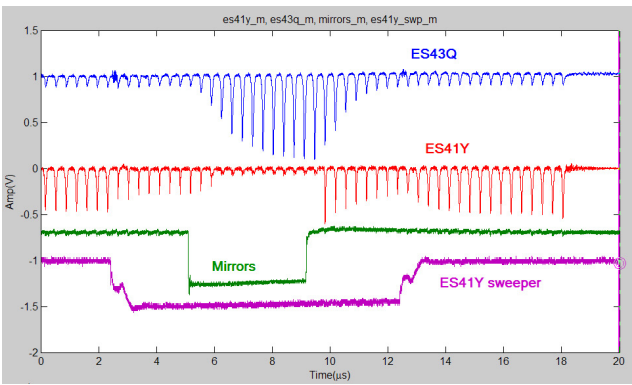

Figure 3: Simultaneous signal traces from an experiment where both the mirrors and the ES41Y (drift space) sweep electrode were pulsed for several μs (data taken 7/1/07).

The ES41Y sweeper clears the gap between bunches in the drift space and reduces the prompt signal ~30%. When the mirrors are pulsed (-2kV) an additional large reduction (factor of ~4) is seen in the ES41Y prompt signal along with a growing signal in the quadrupole.

One problem with a long pulse on the ES41Y sweep electrode is that it can also affect the multipacting process. A better way to clear the gap is to pulse the sweep electrode for a short time <100 ns during the gap passage. In this way the sweep field is absent during the beam pulse and will not affect the trailing edge multipactor. To do this we used a turn-by-turn sequence of 10 pulses timed toward the end of the gap as shown in Fig. 4. Only the first 4 sweep pulses are shown for clarity in Fig. 4. The first sweep pulse clears out the gap and the subsequent prompt pulses are reduced since they are the result of EC generation (multipacting) for just one turn. A comparison of the swept signals after 3 or 4 sweep pulses in Fig. 4 shows a factor ~5 reduction with the mirrors on (red) compared to the case when the mirrors are off (blue) which implies that ~80% of the swept signal is caused by electrons ejected from the nearby quadrupoles..

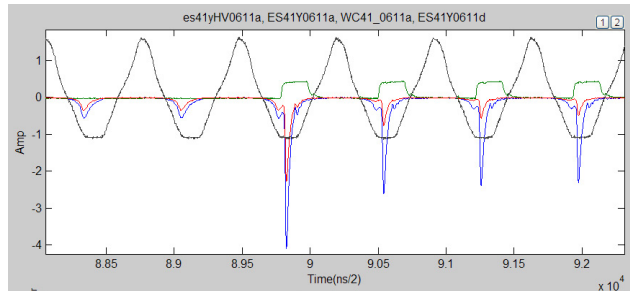

Figure 4: Signals using a turn-by-turn sequence of ES41Y sweep pulses (green). The ES41Y signal with mirrors on (red) is compared with mirror off (blue) and the beam current signal (gray) (data collected 6/11/08).

ES41Y signals at the end of the sequence are shown in Fig. 5 for mirrors on and off. Here the first prompt signal after the last swept gap is down a factor of ~4 when the mirrors are on (red) compared to the situation when the mirrors are off (blue). This implies that a good fraction (~75%) of the prompt signal in the drift space diagnostic is also caused by electrons ejected from the nearby quadrupoles. Note that the prompt and swept pulses are starting to recover after the last sweeper pulse.

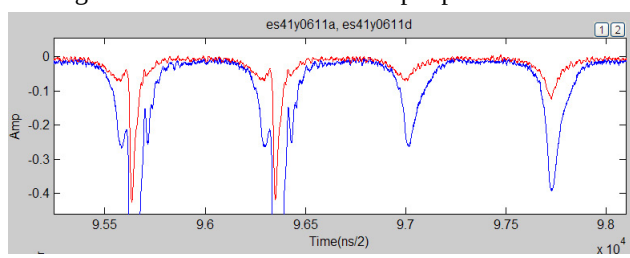

Figure 5: Signals near the end of the 10 turn sequence comparing traces for mirrors off (blue) and mirrors on (red) DC at -2kV (data collected 6/11/08).

These results can help explain some longstanding puzzles such as the null effect of weak solenoids on the e-p instability threshold. Weak magnetic solenoids will suppress trailing edge multipacting, as was observed [7], but will not influence the electrons ejected from the quadrupoles during the beam pulse passage. These will move longitudinally in the drift space and oscillate transversely in the strong potential of the beam where they can still drive the instability. A similar argument holds for TiN, grooved chambers, NEG coatings and other treatments that lower the SEY in drift spaces and thereby suppress multipacting. The electrons ejected from the quadrupoles are not affected by such measures in the drift spaces. To be effective for a long bunch machine the mitigation strategies must be used to suppress EC buildup in the quadrupoles.

The large increase (factor of 5 to 10) in the ES43Q signal when the mirrors are pulsed also occurs when mirror I is biased continuously (DC) at -2kV. The effect has been seen experimentally many times whenever mirror I is biased more than -500V or so. The effect has

not yet been reproduced in simulations which are still a work in progress that do not yet include the beam size (or lattice function) variations between the quadrupole and the mirror.

Simulations

A selected sequence of snapshots of simulated EC generation is shown in Fig. 6, 7, 8, 9 & 10. They were captured at various times in one turn of a multi-turn simulation in a single 3D quadrupole using a modified version of POSINST12.1 [8] with a mirror field added. The selected snapshots were part of an animation (frames 5 ns apart) to show the time evolution of EC generation and electron ejection from a quadrupole plus the effect of a mirror. The full animation is available at ref [9].

The beam intensity used in the simulation was $5x10^{13}$ protons per pulse (8 μC/pulse) and the rms beam size was 4.5mm (horizontal) by 12 mm (vertical). Seed electrons are generated uniformly from Z=0 to 0.9m at the wall and none elsewhere. The proton beam travels in the +Z direction. The graphic on the left plots the electron spatial coordinates with color of the dot related to the total electron velocity as indicated by the color bar; m is the number of macro electrons in the plot. The bottom right graph is a plot of the electron Z coordinate and longitudinal velocity (Vz) while the top right plot shows the beam intensity (red) and electron line density (green) as a function of time. The time of the snapshot from the start of the 1st turn is shown in blue in the upper right plot. In the lower right plot the location in Z of the effective edges of quadrupole are shown in blue and downstream edge of the mirror is shown in gray.

The first snapshot (Fig. 6) is taken at the end of the gap after the 5th turn at the start of the 6th turn. It shows that the pipe in the drift space is filled with low energy electrons at the end of the gap between bunch passages. In the quadrupole region one can see a concentration of electrons trapped along the quadrupole field lines.

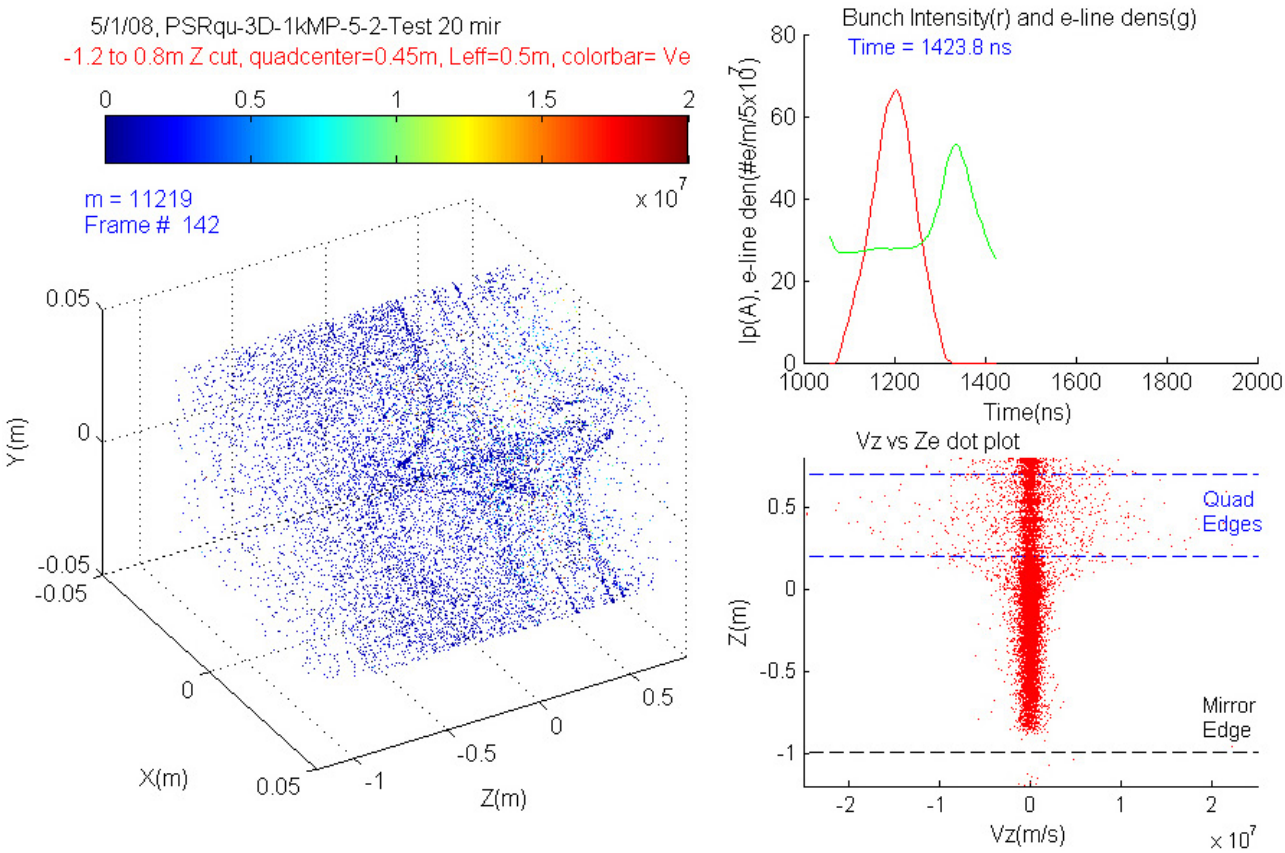

Figure 6: Snapshot at start of 6th turn.

The snapshot of Fig. 7 is taken 50 ns (10 frames) later and shows that electrons in both the drift space and quadrupole are being pinched in a smaller radius by the beam space charge potential. In the lower right plot one can see that a significant number of electrons have been ejected from the quadrupole with negative values of Vz and are traveling upstream towards the mirror.

In Fig. 8 the snapshot is taken 105 ns into the 6th turn just before the first electrons ejected from the quadrupole reach the mirror and somewhat before the peak of the beam pulse. Note that there are a noticeable number of electrons with -Vz $>2x10^7$ m/s, which is a longitudinal energy of > 1.1 keV.

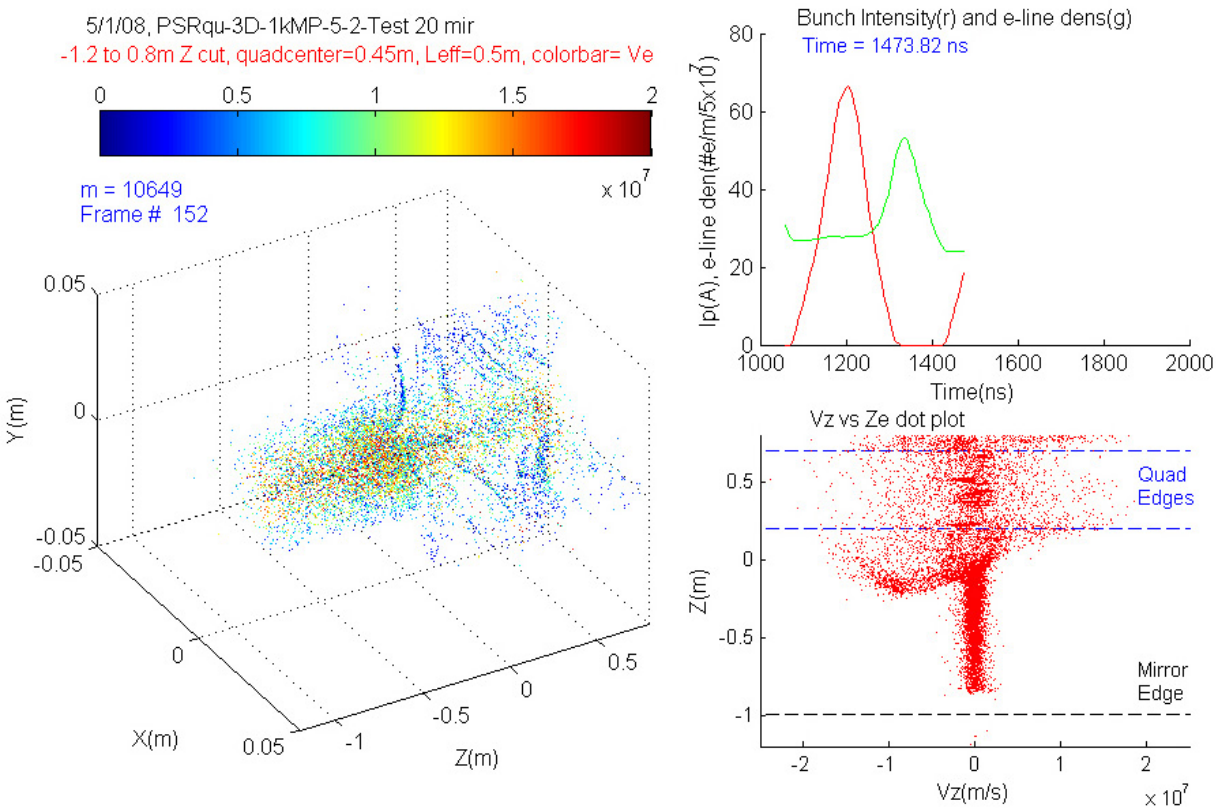

Figure 7: Snapshot 50 ns into the 6th turn.

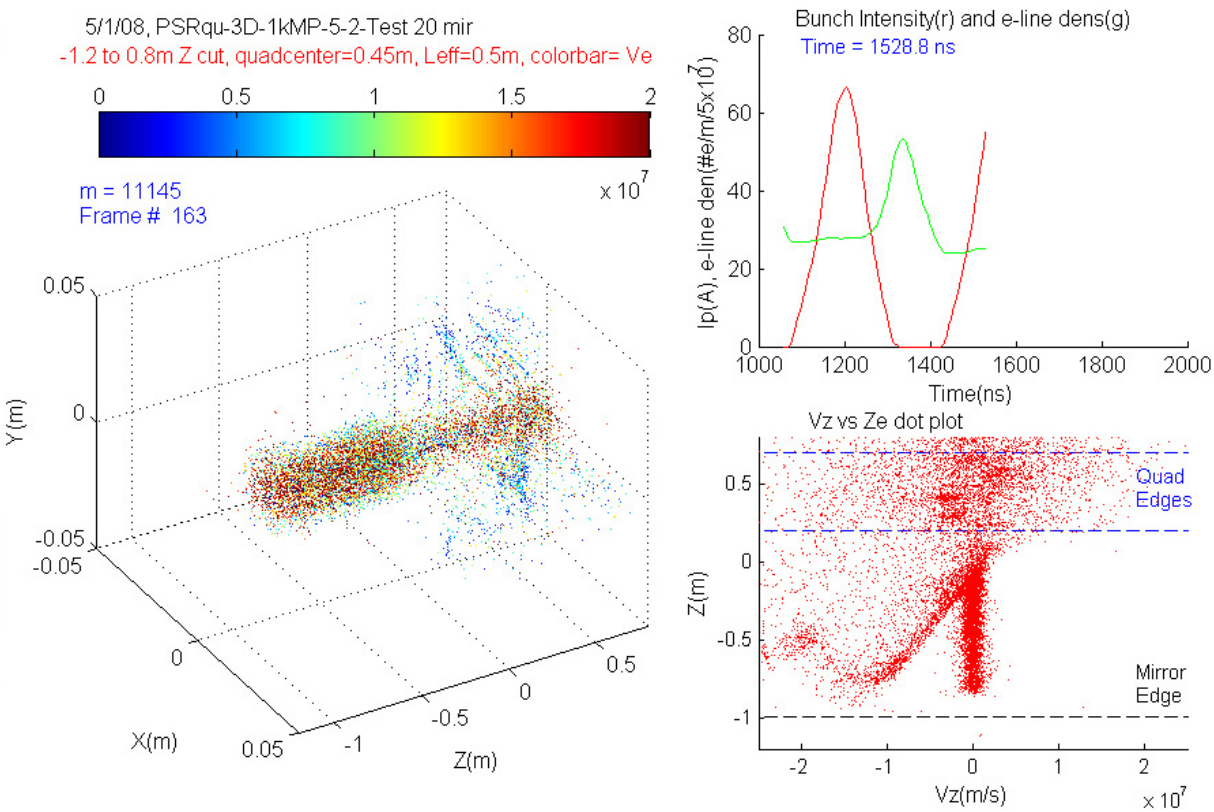

Figure 8: Snapshot 105 ns into the 6th turn.

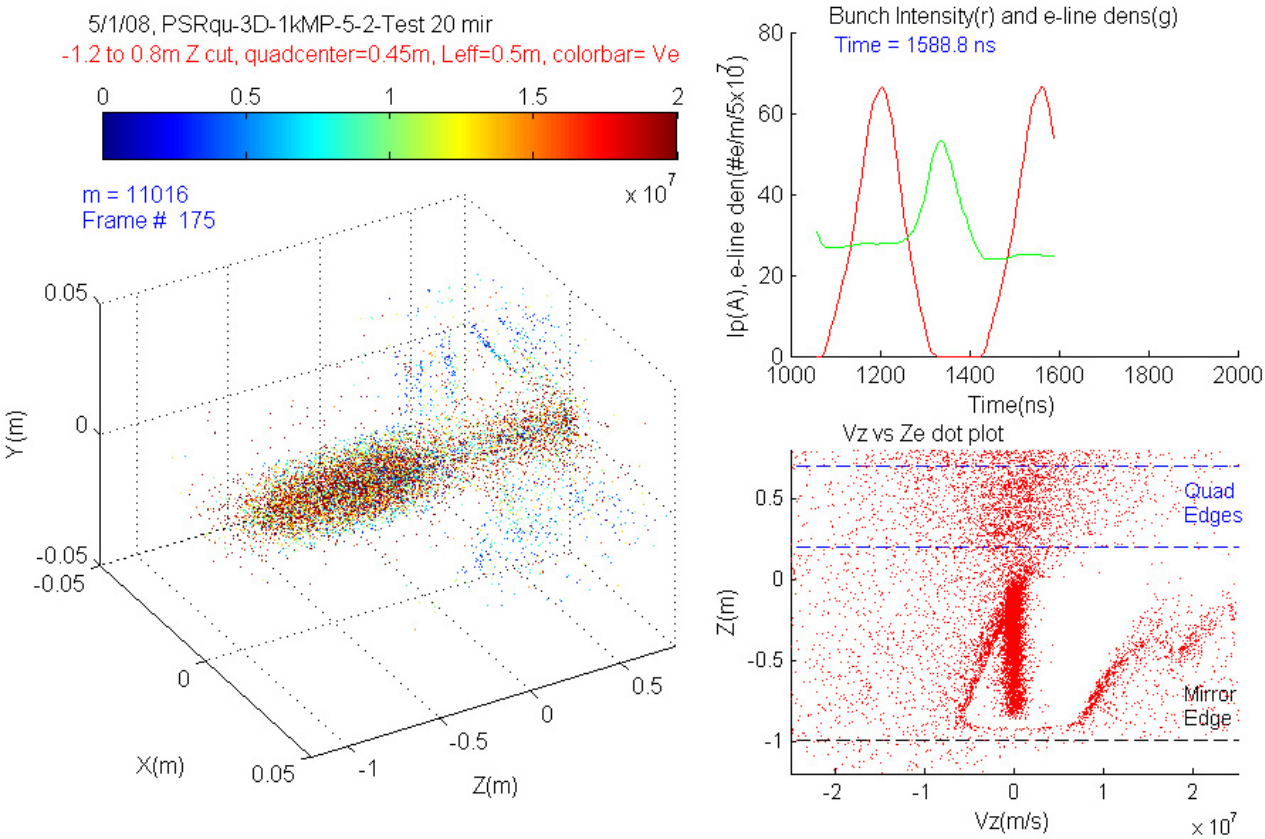

Figure 9: Snapshot 165 ns into the 6th turn and just after the peak of the beam pulse intensity.

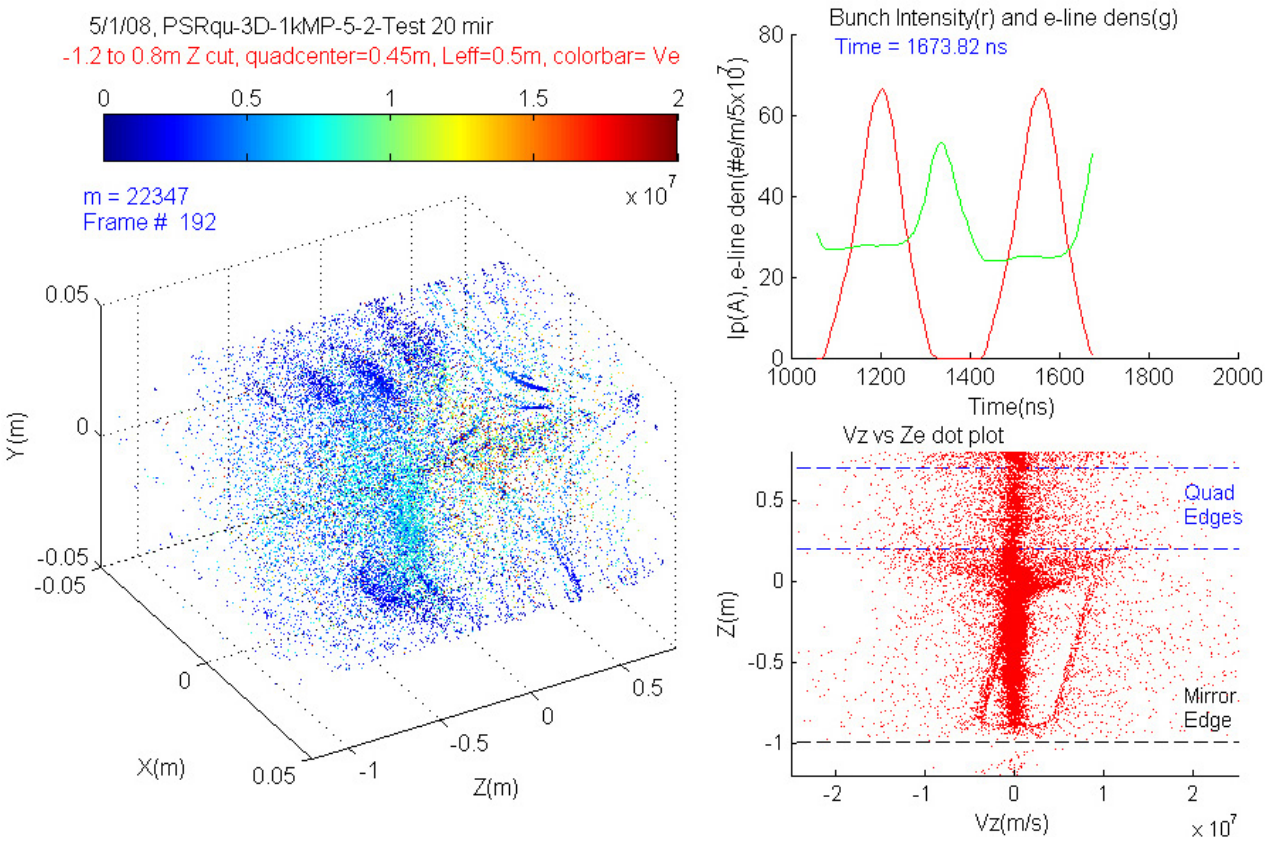

Figure 10: Snapshot at end of 6th turn (250 ns from start of 6th turn).

Fig. 9 was taken just past the peak of the beam pulse for the 6th turn. The electrons in the drift space are pinched into a smaller radius as seen in the left plot while numerous electrons are observed with high negative Vz in the bottom right plot, which indicates that they were ejected from the quadrupole. The electrons with positive Vz (bottom right plot) are the ones with high negative velocity which were reflected by the mirror at an earlier time in the beam pulse and are headed back to the quadrupole.

The first electrons reflected by the mirror have reached the quadrupole and have started to penetrate the fringe field in the snapshot of Fig. 10 taken at the end of the beam pulse for the 6th turn. Electrons ejected by ExB drifts came from the ±45º region around the ±horizontal axes of the quadrupole. They can renter by ExB drifts with +Vz in the ±45º region around the ±vertical axes if some beam E field is still present. Note that the number of macro electrons has doubled at the end of the pulse and once again fill the beam pipe in both the quadrupole and drift space.

CONCLUSIONS

We have confirmed that the e-p instability threshold curves for PSR do not change when foil scattering losses are increased by a factor of 2. This supports the hypothesis that the EC driving the instability saturate for normal beam losses at the intensities studied.

The experiments using electron mirrors convincingly demonstrate that ~75 % of the drift space prompt signal and ~80% of the swept signal are caused by electrons ejected from the nearby quadrupoles. This result, along with the insights from the simulations, can explain the null effect of weak solenoids in selected drift spaces. Electrons are ejected from the quadrupole during the passage of the beam pulse and are captured in the space charge field of the beam in the drift space. They oscillate in the beam potential where they can drive the instability and are not affected by weak solenoid fields or any drift space surface treatment during the bunch passage. To reduce these electrons the suppression needs to be applied at their source in the quadrupoles.

REFERENCES

[1] R. Macek et al, PRSTAB **11**, 010101 (2008).
[2] R. Macek et al, ECLOUD'04, CERN-2005-001, p 63.
[3] R. A. Rosenberg and K. C. Harkay, Nucl. Instrum. Methods Phys. Res. **A453**, 507 (2000).
[4] J. F. O'Hara et al, PAC07, p4117 (2007).
[5] R. Macek et al, PAC03, p 508 (2003).
[6] R. J. Macek & M. T. Pivi, LANL report LA-UR-06-0179 (2005), also report LCC-0160 at http://www-project.slac.stanford.edu/lc/ilc/TechNotes/LCCNotes/lcc_notes_index.htm.
[7] R. Macek, ECLOUD'02, CERN-2002-001, p259.
[8] M. T. F. Pivi & M. A. Furman, PRSTAB **6**, 034201 (2003).
[9] R. J. Macek et al, proceedings HB2008, talk WGA18 slide 17 (2008).